Available online at www.sciencedirect.com
SCIENCE DIRECT
Journal of Organometallic Chemistry 691 (2006) 2319–2326
Journal of Organometallic Chemistry
www.elsevier.com/locate/jorganchem

Solid state-specific and chiral lattice-controlled asymmetric photoisomerization of 3-substituted propyl cobalt complexes, and direct observation of the intermediate complex

Yoshiaki Ohgo *, Kanako Ishida, Yoshito Hiraga, Yoshifusa Arai, Seiji Takeuchi

Department of Applied Life Sciences, Niigata University of Pharmacy and Applied Life Sciences, Higashijima 265-1, Niigata 956-8603, Japan

Received 29 October 2005; received in revised form 23 December 2005; accepted 23 December 2005
Available online 23 February 2006

Abstract

Solid state-specific and chiral lattice-controlled asymmetric photoisomerization of 3-cyanopropyl cobaloxime complexes coordinated with chiral axial ligand, **1a**–**h**, was found to occur with moderate to relatively high enantioselectivities (~91%ee), even though the reaction proceeds through radical species. The enantioselectivities at a lower temperature (−78 °C) are extremely enhanced as compared to those at room temperature, in most cases.

The configuration of the major enantiomer of the isomerized product is predictable from the shape of the reaction cavity, drawn based on the crystal structure of the starting material. The structure (including absolute configuration) of the intermediate 2-cyanopropyl complex was directly observed by X-ray crystallographic analyses of a single-crystal-to-single-crystal reaction of (*S*)-1-cyclohexylethylamine-coordinated 3-cyanopropyl cobaloxime, **1e**.

Keywords: Asymmetric; Photoisomerization; Chiral lattice; Lattice-controlled; Solid-state reaction; Crystalline-state reaction; Alkyl cobaloxime; X-ray structure analysis

1. Introduction

Solid-state (solvent-free) organic and organometallic reactions have attracted much attention, not only from purely chemical interest, but also from the viewpoint of "green and sustainable chemistry" [1]. Since a reactive group of a molecule is surrounded and constrained by other molecules in the solid-state, the reaction proceeds with high selectivity, or a unique reaction can take place which does not proceed in a solution state.

We have previously reported solid state-specific and irreversible photoisomerization [2] and chiral lattice-controlled asymmetric ($\beta \rightarrow \alpha$) photoisomerization of 2-substituted ethyl cobaloxime complexes [3,4].

In an attempt to develop a novel and analogous system, we found that 3-substituted propyl cobaloxime complexes (γ) isomerized to 1-substituted propyl (α) via 2-substituted propyl complexes (β) irreversibly by visible light irradiation in the solid state [5]. The reaction does not proceed in solution and is therefore "solid state-specific" (see Scheme 1).

Here, if the crystal lattice is chiral, asymmetric isomerization is expected to occur. Thus, several 3-cyanopropyl cobaloxime complexes coordinated with chiral axial bases were prepared and solid-state photoisomerization was examined.

2. Results and discussion

2.1. Preparation and solid-state photoreaction

We prepared several 3-cyanopropyl cobaloxime complexes (**1a**–**h**) coordinated with chiral axial ligand (**a**: (*R*)-2-aminobutanol, **b**: (*S*)-phenylalaninol, **c**: (*R*)-1-phenylethylamine, **d**: (*R*)-2-phenylglycinol, **e**: (*S*)-1-cyclohexylethylamine, **f**: (*S*)-1-benzyl-3-aminopyrrolidine, **g**: (*S*)-3-amino-

* Corresponding author. Tel./fax: +81 250 25 5123.
E-mail address: ohgo@niigata-pharm.ac.jp (Y. Ohgo).

0022-328X/$ - see front matter © 2006 Elsevier B.V. All rights reserved.
doi:10.1016/j.jorganchem.2005.12.067

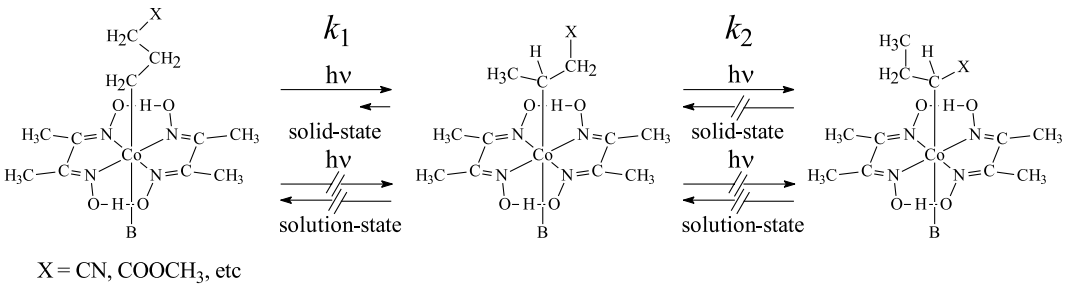

Scheme 1.

pyrrolidine, **h**: (1*S*,2*S*)-2-amino-1-phenyl-1,3-propanediol), which serves as a chiral handle for forming the chiral crystal-lattice, by ligand displacement of aqua, benzylamine or aniline-coordinated 3-cyanopropylcobaloximes with **a**–**h**, and the structures were characterized by IR and NMR spectra.

Powdered samples of these complexes **1a**–**h** were suspended in nujol and irradiated with a Wacom solar simulator (light source of a 500 W Xe lamp with flux density: 100 mW/cm^2) for a certain period of time (shown in Fig. 1). The chiral base was displaced by an achiral ligand, dimethylphenylphosphine (**p**) (Scheme 2), and the sample was analyzed by HPLC using a chiral column (Chiralcel OD–H), to obtain the ratio of dimethylphenylphosphine-coordinated γ complex (**1p**), (*S*) and (*R*)-isomers of β (**2p**) and α (**3p**) complexes. As a representative example, the time courses of the ratios of complexes, **1c**, and the isomerized products (**2c** and **3c**), and the time courses of the enantioselectivities of each isomerized product (**2c** and **3c**) are shown in Figs. 1 and 2, respectively.

As shown in Fig. 1, the ratio of the starting material **1c** decreased very rapidly with time, and shortly after the initiation of the reaction, the ratio of 2-cyanopropyl complex **2c** increased for a short period of time and then began to decrease. Finally, the 1-cyanopropyl complex (α-complex) **3c** appeared, and the ratio increased rapidly with time. After irradiation for 8 h, the ratio of the α-complex reached to 98.1% (at this stage the ratio of β and γ complexes are 0% and 1.9%, respectively). This pattern clearly shows the reaction to be a typical consecutive one. The first-order rate constant ($k_1 = 1.0 \times 10^{-3}\ s^{-1}$) of the first step was obtained from the time course of **1c** at the early stage. Using the first-order rate constant, initial concentration (in ratio) of **1c** (100%) and concentration (in the ratio) of **2c** at time t, we can calculate the rate constant of the second step (k_2) to be $1.6 \times 10^{-2}\ s^{-1}$ [5].

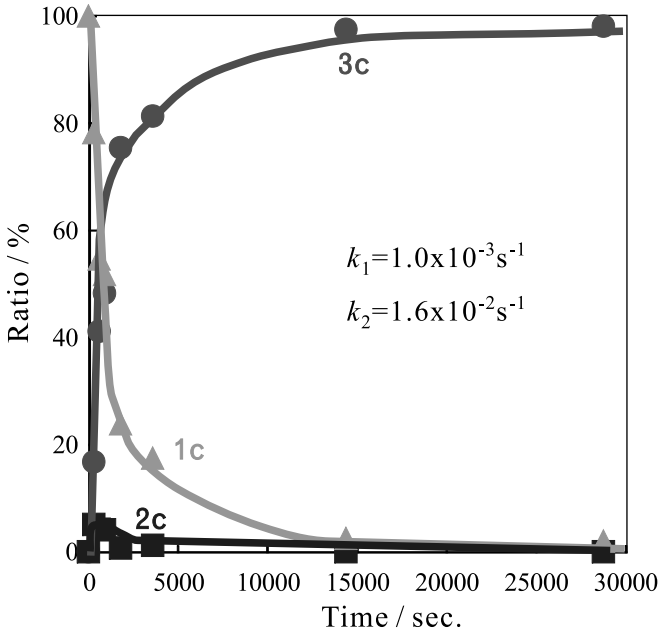

Fig. 1. The time courses of complexes **1c** (▲),**2c** (■), and **3c** (●).

The enantioselectivity of β-complex reached 13.8%ee at 60 min and tended to decrease gradually thereafter. The enantioselectivity of α-complex reached 71.2%ee (maximum) at 240 min and thereafter did not decrease notably.

Other complexes coordinated with other chiral amines were also examined, and the rate constants, maximum enantioselectivities, and the configuration of the major enantiomer produced in each reaction at room temperature are summarized in Table 1.

The configuration of the major enantiomer of the α complex **3c** produced was assumed from the sign of the optical rotation of the final product **3p** [6]. The configuration of the major enantiomer produced in the other reaction was inferred from the correlation of the HPLC data ((*R*)-enantiomer of **3p** travels faster than the (*S*)-enantiomer on HPLC (Chiralcel OD–H) using ethanol/hexane (5/95) as the solvent system). The configuration (at the carbon bonded to cobalt) of the major enantiomer of the β-complex **2e** produced, was assigned by direct observation of the intermediate β-complex by X-ray crystallographic analyses, as described later, and the configuration of the major enantiomer of β-complexes produced in each reaction was assigned by the correlation between the HPLC data of **2p** produced from each reaction and that of **2p** produced from the reaction of **1e**.

Much higher enantioselectivity was expected to be obtained at a lower temperature due to contraction of the crystal lattice. So, we carried out the same reaction at −78 °C. The results are summarized in Table 1. As expected, the enantioselectivity at −78 °C was remarkably enhanced as compared with that at room temperature, in most cases examined. Especially, in the case of (*S*)-phenylalaninol-coordinated complex (**1b**), a dramatic enhancement in enantioselectivity was observed: The enantioselectivity in

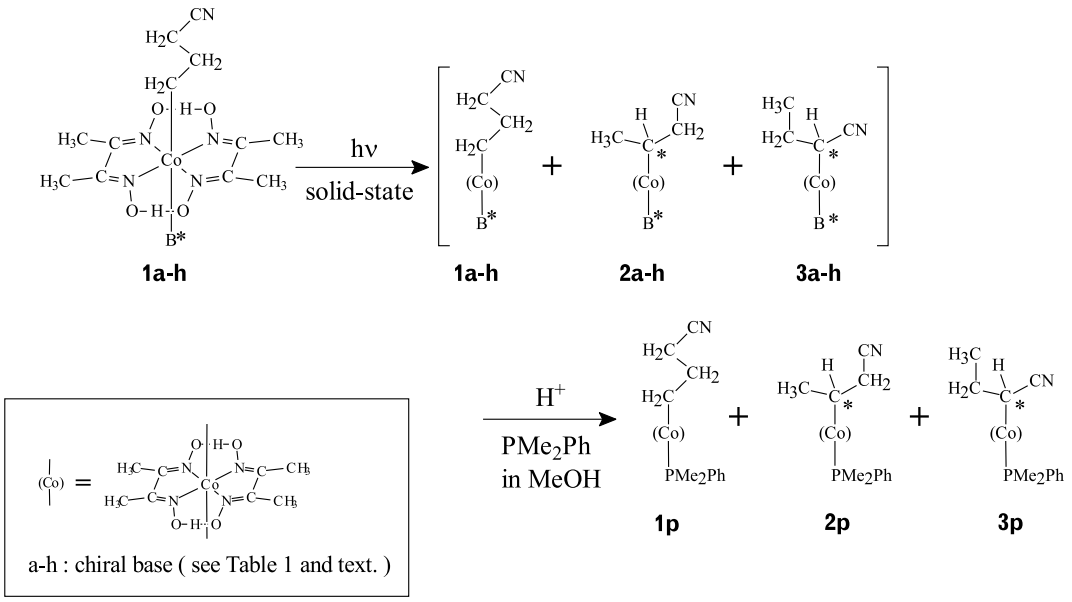

Scheme 2.

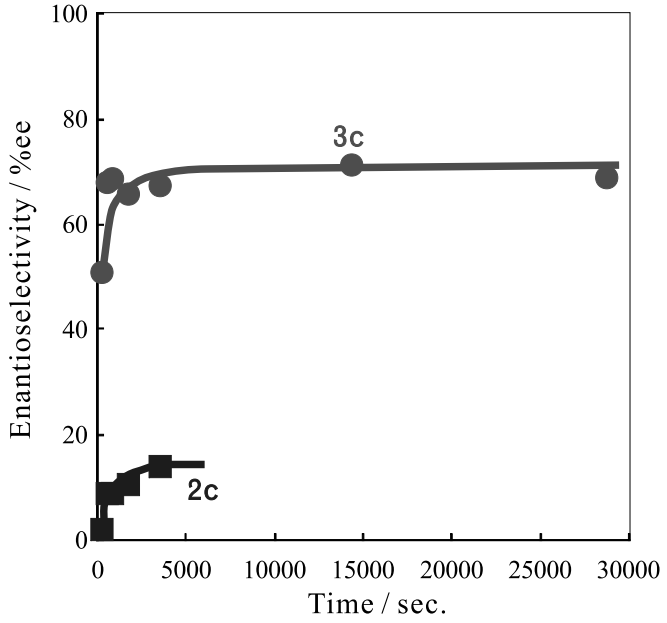

Fig. 2. The time courses of enantioselectivities for **2c** (■) and **3c** (●). **2c** was not detectable at 14400 s. and 28800 s.

α-complex (**3b**) at −78 °C reached 90.9%ee (*R*), while that at room temperature was 34%ee (*R*). In the reaction of **1b** and **1c**, the enantioselectivity of the β-complex (**2b** and **2c**) was also extremely enhanced at −78 °C, as compared with those at room temperature (from 23%ee (*R*)(**2b**) at r.t. to 63.8%ee (*R*)(**2b**) at −78 °C; from 13.8%ee (*S*)(**2c**) at r.t. to 60.7%ee (*R*)(**2c**) at −78 °C).

Asymmetric induction was found to occur in every case here examined. A relatively high degree of enantioselectivities was attained, even though the reaction proceeded through radical species. Generally, the reaction rate in the second step (β → α) is much faster than that in the first step (γ → β).

The enantioselectivity at a lower temperature (−78 °C) is extremely enhanced as compared to that at room temperature.

It is noteworthy that the enantioselectivity (of **2e**) of the first step in the reaction of **1e** is exceptionally high and moreover, there is a period in which the ratio of β-isomer is relatively high. These advantages made it possible to observe an intermediate state directly and also to determine the configuration of the major enantiomer (at the carbon bonded to cobalt) of the intermediate β-complex by X-ray analyses.

2.2. X-ray studies

2.2.1. Mechanism of enantioselection

In order to elucidate the mechanism of enantioselection, we investigated the X-ray crystallographic analysis of **1e**.

The crystal structure and molecular structure of **1e** at −80 °C are shown in Figs. 3 and 4, respectively. Based on the crystal structure, we can describe the reaction cavity where the reactive group can move freely [7].

Fig. 5(a) and (b) are the top view (viewed along the normal to the inplane ligand) and a side view of the cavity (the projection from the side (N(1) and N(4))), respectively.

The nitrogen atom of CN of the β complex is considered to be accommodated almost in the same region as that of the γ-complex, because the methylene group (at β) should work as an adjuster, and the larger methyl group is preferentially located in the wider space (in the direction toward N(4)), and the small hydrogen is also located in the narrow space. Consequently, the major enantiomer of the β complex is expected to have (*R*)-configuration. However, for the α carbon to bind to cobalt, to give the α-complex, rod-like C(α)–C≡N group demand a long-shaped space, and to be nearly parallel to the planar inplane ligand so

Table 1
Rate constants and enantioselectivities in the solid-state photoisomerization of chiral base-coordinated 3-cyanopropyl cobaloximes

Substrate (**1**)		Rate constant (s^{-1})		Enantioselectivity (%ee)[a] (config.)[b]			
Code	B*	r.t.		r.t.		−78 °C	
		k_1	k_2	**2**	**3**	**2**	**3**
1a	(*R*)-2-Aminobutanol	9.9×10^{-5}	1.2×10^{-3}	25.5(*R*)	28.4(*S*)	17.5(*R*)	41.2(*S*)
1b	(*S*)-Phenylalaninol	4.2×10^{-5}	4.9×10^{-4}	23.1(*R*)	34.0(*R*)	63.8(*R*)	90.9(*R*)
1c	(*R*)-1-Phenylethylamine	1.0×10^{-3}	1.6×10^{-2}	13.8(*S*)	71.2(*S*)	60.7(*R*)	52.1(*S*)
1d	(*R*)-2-Phenylglycinol	4.0×10^{-5}	5.8×10^{-4}	5.4(*S*)	51.4(*R*)		
1e	(*S*)-1-Cyclohexylethylamine	9.5×10^{-5}	6.8×10^{-4}	64.1(*R*)	10.2(*S*)	65.4(*R*)	36.0(*S*)
1f	(*S*)-1-Benzyl-3-amino-pyrrolidine	1.6×10^{-4}	3.1×10^{-3}	26.0(*R*)	11.3(*R*)	50.8(*R*)	44.9(*R*)
1g	(*S*)-3-Aminopyrrolidine	6.7×10^{-5}	1.5×10^{-3}	2.5(*R*)	2.9(*R*)		
1h	(1*S*,2*S*)-2-Amino-1-phenyl-1,3-propanediol	5.5×10^{-5}	1.2×10^{-4}	31.8(*R*)	32.6(*S*)	19.7(*R*)	25.4(*S*)

[a] Maximum enantioselectivity.
[b] Configuration of the major enantiomer.

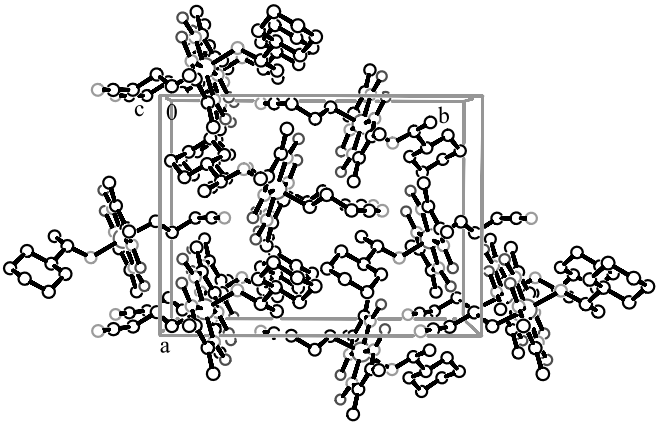

Fig. 3. Crystal structure of **1e**.

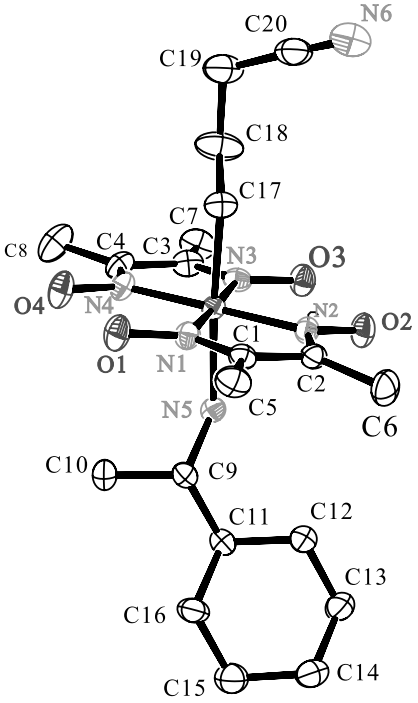

Fig. 4. Molecular structure of **1e**. Hydrogen atoms are omitted for clarity.

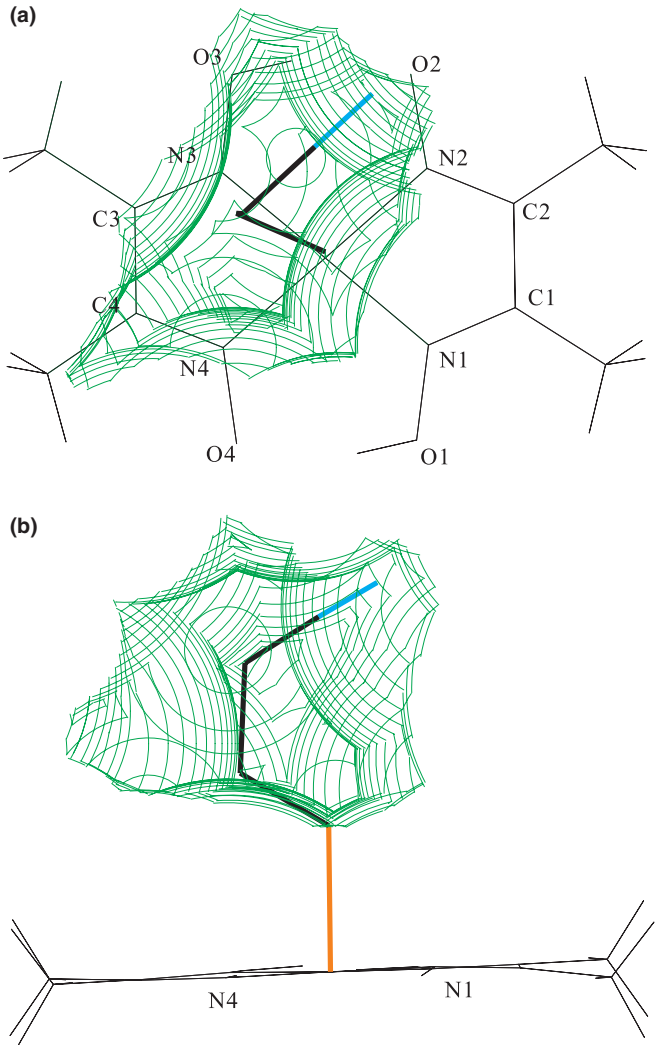

Fig. 5. Top view (a) and side view (b) of reaction cavity and alkyl group drawn based on the crystal structure of **1e**.

that the cyano group cannot make a parallel movement toward the in-plane ligand from the original position, because there is not enough room in this region. Consequently, the cyano group must make fairly large movements. C(α)–C≡N should be directed toward C(4) for

meeting the long-shaped and rod-like steric demand. In this situation, the ethyl group is favored to locate in the space toward O(2) and N(2), then, the configuration becomes *S*, which is consistent with the result (see Table 1). The configuration of the major enantiomer of **3c** is also predictable from the shape of the reaction cavity of **1c**, drawn based on the crystal structure [8].

Thus, the configuration of the major enantiomer (of α and β isomers) produced, was found to be predictable from the shape of the reaction cavity, drawn based on the crystal structure of the starting material.

2.2.2. Direct observation of intermediate β-complex in a single crystal-to-single crystal reaction

We have previously found and reported many examples of crystalline state racemization of chiral alkyl coordinated cobaloxime complexes in which the crystal lattice does not collapse during the reaction [7,9]. We expected that the present reaction would also proceed without degradation of crystallinity.

In order to prove the hypothetical movement of alkyl in the process of the isomerization of **1e**, and the inferred mechanism for the configurational reversal of the major enantiomer between the first and second steps, we tried to observe directly the movement of the alkyl group with the reaction time by X-ray crystallographic analysis.

The crystallographic data and final *R* factors obtained by crystal structure analyses of samples irradiated for 10 and 20 h at −78 °C indicated that the crystals still maintained good crystallinity, enough to enable crystal structure analysis even after irradiation.

Molecular structure and reaction cavity obtained by structural analysis at irradiation time (20 h) are shown in Figs. 6 and 7.

After 10 h of irradiation, the 2-cyanopropyl (the intermediate β-complex) appeared, though the occupancy was only 15%. The intermediate β-complex was clearly observed in an occupancy factor of 36% in the molecular structure obtained (by structural analysis) after 20 h of irradiation. The cavity at the same stage as the molecular structure shows that the cyano nitrogen of the β-complex produced is situated in almost the same region as in the original, as predicted previously. C(α)–C≡N turned nearly vertical toward the in-plane ligand, and the methyl group of β-cyanopropyl is located in the region directed toward N(4) from the cobalt atom, as expected previously. Thus, the configuration of the major enantiomer of β-complex (**2e**) was proved to be *R* which was consistent with the predicted one.

At present, we could not observe **3e** in the single-crystal-to-single-crystal reaction of **1e**. Two factors, described below, are considered to operate synergetically, which would be the reason why we could not observe **3e** in the reaction using single crystal at −78 °C: (1) The reaction rates in the crystalline-state are usually 1 order lower than those in the solid-state reactions using a finely powdered sample. (2) The reaction rate of the second step (k_2) at a lower temperature (−78 °C) is extremely decreased in the isomerization of **1e**. Further investigation along this line is now being undertaken.

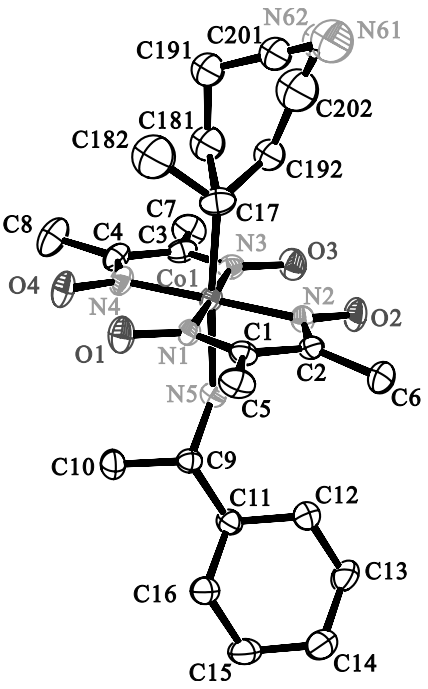

Fig. 6. Molecular structure of **1e** (after 20 h of irradiation). Hydrogen atoms are omitted for clarity. 2-Cyanopropyl, C(182)–C(17)–C(192)–C(202)–N(62), appears clearly in occupancy factor of 36%. The figure shows that 2-cyanopropyl has (*R*)-configuration.

3. Experimental

3.1. General

^{1}H NMR spectra were recorded on JEOL JNM- α400 and BRUKER BIOSPIN AVANCE DPX250 spectrometers, using TMS as the internal standard. IR spectra were recorded on a JASCO FT/IR-460 PLUS spectrometer. Optical rotations were measured on a Perkin–Elmer 241 polarimeter. A WACOM Solar Simulator WX-105H (Xe lamp with Flux density: 100 mW/cm^2) was used as a light source for photoreactions. Microanalyses were performed on a Perkin–Elmer 240-002 and CE INSTRUMENTS EA1110.

*3.2. Preparation of substrates (**1a–h**)*

Substrates (**1a**–**h**) were prepared basically according to the method described in a previous paper [5], except for using chiral base in axial ligand displacement.

A typical procedure of ligand displacement: 1.347 g (2.99 mmol) of (aniline)(3-cyanopropyl)bis(dimethylglyoximato)cobalt(III) was dissolved in methanol (40 ml). To the solution 5 g of an ion exchange resin (Dowex 50W-X2) and water (10 ml) were added. The reaction mixture was stirred at room temperature. The degree of axial ligand displacement

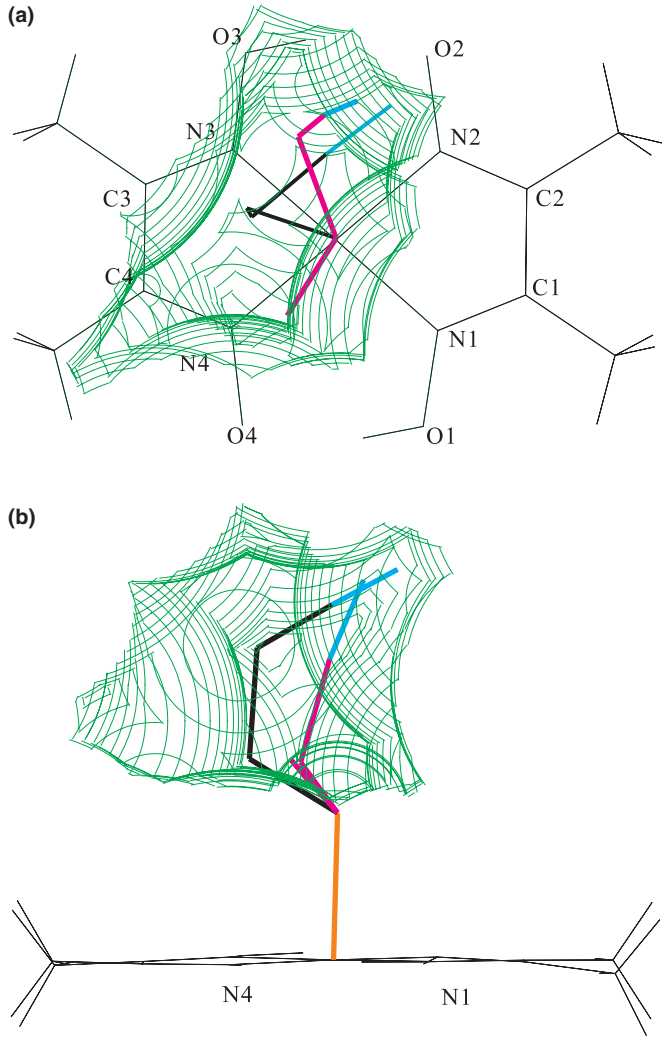

Fig. 7. Top view (a) and side view (b) of reaction cavity and alkyl groups drawn based on the crystal structure of **1e** (after 20 h of irradiation). Hydrogen atoms of the alkyl groups are omitted for clarity. Black line and red line are carbon skeletons of the original 3-cyanopropyl and the isomerized 2-cyanopropyl group, respectively. Cyano nitrogen of each alkyl is colored with blue. (For interpretation of the references to colour in this figure legend, the reader is referred to the Web version of this article).

with aqua was monitored by TLC. After completion of the ligand displacement, the reaction mixture was filtered. 0.39 ml (1.02 eq) of (*R*)-1-phenylethylamine was added to the filtrate with stirring. Ligand exchange reaction of aqua with the amine was monitored by TLC. After completion of the reaction, the solution was evaporated to dryness under a reduced pressure. The crude product was recrystallized from ethyl acetate (70 ml) and hexane (140 ml) to give 0.111 g of orange crystals of **1c**. From the filtrate, another 0.61 g of crystals was obtained. The filtrate was evaporated to dryness under a reduced pressure to give 0.498 g of crystals from which 0.096 g of crystals (**1c**) was also obtained by the same recrystallization procedure as above. Total yield: 0.818 g (57.1%).

^{1}H NMR, IR, and microanalyses data of several key substrates are described as follows. **1a**: ^{1}H NMR(400 MHz, $CDCl_3$): δ 3.63(dd, 1H, $J = 3.8$ and 11.4 Hz, –CH–O of aminobutanol), 3.22(dd, 1H, $J = 6.1$ and 11.4 Hz, –CH–O of aminobutanol), 2.34(m, 1H, –NH), 2.25(s, 6H, CH_3 of dimethylglyoxime), 2.24(s, 6H, CH_3 of dimethylglyoxime), 2.23(m, 1H, N–CH– of aminobutanol), 2.21(broad, 1H, –OH of aminobutanol), 2.18(t, 2H, $J = 7.2$ Hz, –CH_2–CN), 1.67(m, 1H, –NH of aminobutanol), 1.43–1.14(m, 6H, –C–CH_2–C of aminobutanol, Co–CH_2–, and Co–C–CH_2–), 0.77(t, 3H, $J = 7.5$ Hz, –C–CH_3 of aminobutanol). IR(KBr): 3459.7, 3293.3, 3244.7, 2238.0, 1569.8, 1228.4, and 1069.8 cm^{-1}. Anal. Calc. for $C_{16}H_{31}CoN_6O_5$: C, 43.05; H, 7.00; N, 18.83. Found: C, 42.77; H, 7.29; N 18.53%. **1b**: ^{1}H NMR(250 MHz, $CDCl_3$): δ 7.30(m, 3H, aromatic), 7.02(m, 2H, aromatic), 3.56(dd, 1H, $J = \sim 1.0$ and 10.0 Hz, –CH–O of phenylalaninol), 3.34(dd, 1H, $J = 2.8$ and 10.0 Hz, –CH–O of phenylalaninol), 2.60(s, 3H, N–CH–CH_2– of phenylalaninol), 2.30(m, 1H, –NH of phenylalaninol), 2.19(s, 6H, CH_3 of dimethylglyoxime), 2.16(m, 2H, –CH_2–CN), 2.14(s, 6H, CH_3 of dimethylglyoxime), 2.00(broad, 1H, –OH of phenylalaninol), 1.71(m, 1H, –NH of phenylalaninol), 1.33(m, 2H, Co–CH_2–), 1.14 (m, 2H, Co–C–CH_2–). IR(KBr): 3331.4, 3292.9, 3244.2, 2237.0, 1559.2, 1222.7, 1085.2, 746.8, and 704.9 cm^{-1}. Anal. Calc. for $C_{21}H_{33}CoN_6O_5$: C, 49.61; H, 6.54; N, 16.53. Found: C, 49.89; H, 6.70; N, 16.23%. **1c**: ^{1}H NMR(400 MHz, $CDCl_3$): δ 7.29(m, 3H, aromatic), 7.08(m, 2H, aromatic), 3.69(tq, 1H, $J = 6.3$ and 6.3 Hz, –N–CH– of phenylethylamine), 2.44(m, 1H, –NH of phenylethylamine), 2.156(t, 2H, $J = 7.2$ Hz, –CH_2–CN), 2.151(s, 6H, CH_3 of dimethylglyoxime), 2.149(s, 6H, CH_3 of dimethylglyoxime), 1.72(m, 1H, –NH of phenylethylamine), 1.35(m, 2H, Co–CH_2–), 1.26(d, 3H, $J = 6.8$ Hz, CH_3 of phenylethylamine), 1.16 (m, 2H, Co–C–CH_2–). IR(KBr): 3321.8, 3273.1, 2246.7, 1564.5, 1235.2, 1077.1, 769.5, 761.3 and 702.4 cm^{-1}. Anal. Calc. for $C_{20}H_{31}CoN_6O_4$: C, 50.21; H, 6.53; N, 17.57. Found: C, 50.48; H, 6.79; N, 17.60%. **1d**: ^{1}H NMR(250 MHz, $CDCl_3$): δ 7.30(m, 3H, aromatic), 7.08(m, 2H, aromatic), 3.78(m, 1H, N–CH– of phenylglycinol), 3.62(dd, 1H, $J = 3.9$ and 11.5 Hz, –CH–O– of phenylglycinol), 3.15(dd, 1H, $J = 9.8$ and 11.5 Hz, –CH–O– of phenylglycinol), 2.76(d, 1H, $J = 11.1$ Hz, –NH of phenylglycinol), 2.48(t, 1H, $J = 10.9$ Hz, –NH of phenylglycinol), 2.42(broad, 1H, –OH of phenylglycinol), 2.14(t, 2H, $J = 7.0$ Hz, –CH_2–CN), 2.01(s, 6H, CH_3 of dimethylglyoxime), 2.00(s, 6H, CH_3 of dimethylglyoxime), 1.30(m, 2H, Co–CH_2–), 1.13(m, 2H, Co–C–CH_2–). IR(KBr): 3314.6, 3247.1, 2238.0, 1559.2, 1230.8, 1088.1, 1056.3, 760.8, and 703.4 cm^{-1}. Anal. Calc. for $C_{20}H_{31}CoN_6O_5$: C, 48.59; H, 6.32; N, 17.00. Found: C, 48.57; H, 6.46; N, 16.87%. **1e**: ^{1}H NMR(250 MHz, $CDCl_3$): δ2.25(s, 12H, CH_3 of dimethylglyoxime), 2.17(t, 2H, $J =$ 7.0 Hz, –CH_2–CN), 2.15–0.65(m, 13H, –C_6H_{11} and –NH_2 of cyclohexylethylamine), 2.08(m, 1H, N–CH– of cyclohexylethylamine), 1.34(m, 2H, Co–CH_2–), 1.15(m, 2H, Co–C–CH_2–), 0.86(d, 3H, $J = 6.6$ Hz, N–C–CH_3 of cyclohexylethylamine). IR(KBr): 3314.6, 3252.8, 2922.6, 2239.0,

1563.0, 1235.7, and 1093.4 cm^{-1}. Anal. Calc. for $C_{20}H_{37}CoN_6O_4$: C, 49.58; H, 7.70; N, 17.35. Found: C, 49.41; H, 7.64; N, 17.21%. **1f**: ^{1}H NMR(400 MHz, $CDCl_3$): δ 7.28(m, 3H, aromatic), 7.21(m, 2H, aromatic), 3.55(d, 1H, $J = 12.8$ Hz, N–C*H*–Ph of 1-benzyl-3-aminopyrrolidine), 3.45(d, 1H, $J = 12.8$ Hz, N–C*H*–Ph of 1-benzyl-3-aminopyrrolidine), 2.92(m, 1H, H-3 of 1-benzyl-3-aminopyrrolidine), 2.79(dt, 1H, $J = 3.3$ and 8.7 Hz, H-5 of 1-benzyl-3-aminopyrrolidine), 2.37(m, 1H, H-2 of 1-benzyl-3-aminopyrrolidine), 2.24(dd, 1H, $J = 6.0$ and 10.4 Hz, H-2′ of 1-benzyl-3-aminopyrrolidine), 2.20(s, 6H, CH_3 of dimethylglyoxime), 2.19(s, 6H, CH_3 of dimethylglyoxime), 2.15(t, 2H, $J = 7.1$ Hz, –CH_2–CN), 2.15–2.00(m, 3H, –NH, H-4, and H-5′ of 1-benzyl-3-aminopyrrolidine), 1.93(m, 1H, –NH of 1-benzyl-3-aminopyrrolidine), 1.34(m, 1H, H-4′ of 1-benzyl-3-aminopyrrolidine), 1.31(m, 2H, Co–CH_2–), 1.15(m, 2H, Co–C–CH_2–). IR(KBr): 3479.9, 3270.2, 3242.7, 2247.2, 1565.4, 1235.2, 1088.1, 755.0, and 706.8 cm^{-1}. Anal. Calc. for $C_{23}H_{36}CoN_7O_4 \cdot H_2O$: C, 50.09; H, 6.94; N, 17.78. Found: C, 50.19; H, 6.87; N, 17.79%.

3.3. A typical procedure for the photoreactions and the subsequent analytical consequences

In a typical experiment, 51.4 mg of crystals, **1c**, was suspended in 2.5 ml of nujol and powdered by a grinder for 10 min. The suspended sample was transferred into a petri-dish with 8.8 cm-diameter and a trace amount of the residue left on the dish was washed two times with another 2 ml of nujol, and was transferred into the same petri-dish. The sample suspended in nujol was irradiated with a solar simulator (Flux density: 100 mW/cm^2) for 28800 s (8 h). The reaction products were filtered, and the nujol was washed out with hexane to give 39.5 mg of crystals. To crystals were added 30 ml of methanol, 0.5 ml of 6 N HCl, and 0.018 ml (1.5 eq) of dimethylphenylphosphine. The resulting solution was stirred and the reaction was monitored by TLC. After the completion of the ligand displacement, the reaction mixture was neutralized by a $NaHCO_3$ solution and was evaporated to dryness under a reduced pressure. To the residue water was added and the mixture was extracted with methylene chloride. The methylene chloride solution was applied to a silica-gel column and developed with a mixed solvent [ethyl acetate/hexane (1/1)]. The eluate was concentrated to dryness under a reduced pressure to give 40 mg of crystalline solid. The sample was analyzed by HPLC using Chiralcel OD–H (solvent system: ethanol/hexane (5/95)). The data showed the ratio (and enantioselectivity) of **1p**:**2p**:**3p** to be 1.93:0:98.07 (68.7%ee, rich in (*S*)-enantiomer), respectively. $[\alpha]_{589}$ −31.5° (c 0.213, $CHCl_3$, 15.5 °C), $[\alpha]_{578}$ −32.9° (c 0.213, $CHCl_3$, 15.5 °C). The HPLC data for the sample, obtained by treating the reaction products after 14400 s (4 h) of irradiation with the same procedure as above, showed the ratio (and enantioselectivity) of **1p**:**2p**:**3p** to be 2.49:0:97.51 (71.2%ee, rich in (*S*)-enantiomer), respectively.

3.3.1. Preparation and ^{1}H NMR, IR and microanalyses data for *1p*, *2p*, and *3p*

Dimethylphenylphosphine-coordinated 3-cyanopropyl, 2-cyanopropyl and 1-cyanopropyl cobaloxime complexes (**1p**, **2p** and **3p**) used as the authentic samples for the quantitative analysis were prepared by ligand displacement of the corresponding aniline- or benzylamine-coordinated cobaloxime complexes with dimethylphenylphosphine according to the same procedure described in the previous Section 3.2 and also in a previous report [5]. ^{1}H NMR, IR and microanalysis data are described as follows. **1p**: H NMR(400 MHz, $CDCl_3$): δ 7.36(m, 3H, aromatic), 7.10 (m, 2H, aromatic), 2.19(t, 2H, $J = 7.4$ Hz, –CH_2–CN), 1.94(d, 12H, $J_{H-P} = 3.4$ Hz, CH_3 of dimethylglyoxime), 1.53(m, 2H, Co–CH_2–), 1.39(d, 6H, $J_{H-P} = 9.1$ Hz, CH_3 of PMe_2Ph), 1.28(m, 2H, Co–C–CH_2–). IR(KBr): 2902.8, 2239.0, 1558.7, 1234.2, 1091.0, 743.4, and 691.8 cm^{-1}. Anal. Calc. for $C_{20}H_{31}CoN_5O_4P$: C, 48.49; H, 6.31; N, 14.14. Found: C, 48.61; H, 6.43; N, 13.89%. **2p**: ^{1}H NMR(400 MHz, $CDCl_3$): δ 7.36(m, 3H, aromatic), 7.09(m, 2H, aromatic), 2.45(ddd, 1H, $J = 4.4$ and 6.6 Hz, $J = 17.1$ Hz, –CH–CN), 1.99(ddd, 1H, $J = 2.9$ and 9.3 Hz, $J = 17.1$ Hz, –CH–CN), 1.95(d, 6H, $J_{H-P} = 2.7$ Hz, CH_3 of dimethylglyoxime), 1.94(d, 6H, $J_{H-P} = 3.2$ Hz, CH_3 of dimethylglyoxime), 1.37(d, 6H, $J_{H-P} = 9.3$ Hz, CH_3 of PMe_2Ph), 1.24(m, 1H, Co–CH–), 0.81(dd, 3H, $J = 7.1$ Hz, $J_{H-P} = 7.1$ Hz, Co–C–CH_3). IR(KBr): 2850.8, 2229.3, 1550.5, 1233.3, 1093.0, 908.8, 751.6, and 696.7 cm^{-1}. Anal. Calc. for $C_{20}H_{31}CoN_5O_4P$: C, 48.49; H, 6.31; N, 14.14. Found: C, 48.52; H, 6.31; N, 14.10%. **3p**: ^{1}H NMR(400 MHz, $CDCl_3$): δ 7.41(m, 3H, aromatic), 7.14(m, 2H, aromatic), 2.06(m, H, Co–CH–CN), 2.03(d, 6H, $J = 4.0$ Hz, CH_3 of dimethylglyoxime), 2.02(d, 6H, $J = 2.6$ Hz, CH_3 of dimethylglyoxime), 1.420(d, 3H, $J = 10.6$ Hz, CH_3 of PMe_2Ph), 1.417(d, 3H, $J = 12.0$ Hz, CH_3 of PMe_2Ph), 1.14–0.92(m, 2H, Co–C–CH_2–), 0.96(m, 3H, Co–C–C–CH_3). IR(KBr): 2959.7, 2195.6, 1555.8, 1234.7, 1090.1, 910.2, 749.7, and 693.3 cm^{-1}. Anal. Calc. for $C_{20}H_{31}CoN_5O_4P$: C, 48.49; H, 6.31; N, 14.14. Found: C, 48.40; H, 6.18; N, 14.16%.

3.4. X-ray crystallographic studies

Tables of atomic coordinates, anisotropic thermal parameters, bond lengths and angles of **1e** and **1e** (after 20 h of irradiation) may be obtained free of charge from The Director CCDC, 12 Union Road, Cambridge CB2 1 EZ, UK, on quoting the deposition numbers CCDC 286804 and 286805, the names of authors and the journal citation (http://www.ccdc.cam.ac.uk). The procedures of crystal structure determination for both **1e** and **1e** (after 20 h of irradiation) were the same. X-ray data were collected at 173 K on a Rigaku AFC7R four circle diffractometer [10] using Mo Kα X-ray (0.71069) source and a graphite monochromator. The unit cell dimensions were obtained from a least-squares fit to setting angles of 25 reflections. ψ scan absorption corrections were applied

[11]. The structures were solved by direct methods using SIR97 [12] for **1e** and MITHRIL for **1e** (after 20 h of irradiation) [13] and refined by full-matrix least-square method using shelxl97 [14]. In the final step of the refinement procedure, all non-hydrogen atoms were refined with anisotropic displacement parameters for **1e**. For **1e** (after 20 h of irradiation), cyanoalkyl groups bound to cobalt directly were disordered in two parts, (C181, C191, C201 and N61) and (C182, C192, C202 and N62) with refined occupancies of 0.635 and 0.365. Non-hydrogen atoms in the disordered cyanoalkyl groups were refined with isotropic displacement parameters. The other non-hydrogen atoms were refined with anisotropic displacement parameters. All hydrogen atoms were placed in calculated positions and included in the final least squares refinement with a riding model. **1e**: $C_{20}H_{37}CoN_6O_4$, $a = 12.521(2)$ Å, $b = 16.775(8)$ Å, $c = 11.323(2)$ Å, orthorhombic $P2_12_12_1$, $Z = 4$, crystal size (mm) $= 0.27 \times 0.18 \times 0.13$, $T = 193$ °K, θ range for data collection (°) $= 2.71$–27.49, index ranges $h = -16 \rightarrow 16$, $k = -21 \rightarrow 21$, $l = -14 \rightarrow 14$, reflections collected/unique $[R_{int}] = 7531/5448$ [0.0565], $R_1 = 0.0428(I > 2\sigma(I))$, $R_1 = 0.0902$(all), $wR = 0.1184$(all), goodness-of-fit $= 1.119$, Flack χ parameter $= -0.03(2)$. **1e** (after 20 h of irradiation): $C_{20}H_{37}CoN_6O_4$, $a = 12.563(1)$ Å, $b = 16.749(2)$ Å, $c = 11.382(3)$ Å, orthorhombic $P2_12_12_1$, $Z = 4$, crystal size (mm) $= 0.25 \times 0.22 \times 0.22$, $T = 193$ °K, θ range for data collection (°) $= 2.71$–27.49, index ranges $h = -9 \rightarrow 16$, $k = 0 \rightarrow 21$, $l = 0 \rightarrow 14$, reflections collected/unique $[R_{int}] = 3618/3466$ [0.0258], $R_1 = 0.0339(I > 2\sigma(I))$, $R_1 = 0.0539$(all), $wR = 0.0948$(all), goodness-of-fit $= 1.309$, Flack χ parameter $= -0.00(2)$.

Acknowledgements

This work was partly supported by Grant-in-Aids for Scientific Research from the Ministry of Education, Science, Sports and Culture, Japan, and also a Grant-in-Aid for Scientific Research (C) from Japan Society for the Promotion of Science. The authors are grateful to Ms. Yukie Suzuki for preparation of substrates and her technical assistance.

References

[1] K. Tanaka, F. Toda, Chem. Rev. 100 (2000) 1025–1074.
[2] Y. Ohgo, S. Takeuchi, Chem. Commun. (1985) 21–22.
[3] Y. Ohgo, Y. Arai, M. Hagiwara, S. Takeuchi, H. Kogo, A. Sekine, H. Uekusa, Y. Ohashi, Chem. Lett. (1994) 715–716.
[4] Y. Ohgo, M. Hagiwara, M. Shida, Y. Arai, S. Takeuchi, Mol. Cryst. Liq. Cryst. 277 (1996) 241–246.
[5] Y. Ohgo, F. Kurashima, Y. Hiraga, K. Ishida, N. Takatsu, Y. Arai, S. Takeuchi, Chem. Lett. (2001) 1190–1191.
[6] Y. Ohgo, S. Takeuchi, Y. Natori, J. Yoshimura, Y. Ohashi, Y. Sasada, Bull. Chem. Soc. Jpn. 54 (1981) 3095–3099.
[7] The reaction cavity is defined as a space limited by a concave surface of the spheres of surrounding atoms. The radius of each sphere (of the atom) is taken to be 1.2 Å greater than the van der Waals radius of the corresponding atom. See references cited below. (a) Y. Ohashi, K. Yanagi, T. Kurihara, Y. Sasada, Y. Ohgo, J. Am. Chem. Soc. 103 (1981) 5805–5812;
(b) Y. Ohashi, A. Uchida, Y. Sasada, Y. Ohgo, Acta Crystallogr. B 39 (1983) 54.
[8] Preliminary X-ray result of **1c** is briefly described in the Proceedings of ICCOSS XIII; A. Sekine, M. Yoshiike, Y. Ohashi, K. Ishida, Y. Arai, Y. Ohgo, Mol. Cryst. Liq. Cryst. 313 (1998) 321–326, The detailed results will be published later.
[9] Y. Ohashi, Y. Sakai, A. Sekine, Y. Arai, Y. Ohgo, N. Kamiya, H. Iwasaki, Bull. Chem. Soc. Jpn. 68 (1995) 2517, and references cited therein.
[10] MSC/AFC Diffractometer Control Software, Molecular Structure Corporation, MSC, 3200 Research Forest Drive, The Woodlands, TX 77381, USA.
[11] A.C.T. North, D.C. Phillips, F.S. Mathews, Acta Cryst. A 24 (1968) 351.
[12] A. Altomare, M.C. Burla, M. Camalli, G. Cascarano, C. Giacovazzo, A. Guagliardi, A.G.G. Moliterni, G. Polidori, R. Spagna, J. Appl. Cryst. 32 (1999) 115.
[13] C.J. Gilmore, J. Appl. Cryst. 17 (1984) 42.
[14] G.M. Sheldrick, Shelxl97 Program for the Refinement of Crystal Structures, University of Göttingen, Germany, 1997.